EPJ Web of Conferences **123**, 04007 (2016)
Heavy Ion Accelerator Symposium 2015
DOI: 10.1051/epjconf/201612304007

Decay spectroscopy with Solenogam at the ANU Heavy Ion Accelerator Facility

M. S. M. Gerathy[1,a], M. W. Reed[1], G. J. Lane[1], T. Kibédi[1], S. S. Hota[1], and A. E. Stuchbery[1]

[1] *Department of Nuclear Physics, Research School of Physics and Engineering, The Australian National University, Canberra, ACT 2601, Australia*

Abstract. Solenogam is a recoil spectrometer designed and constructed for use at the Australian National University (ANU) Heavy-Ion Accelerator Facility (HIAF). The design enables the study of nuclear excitations populated by the decay of long-lived states such as isomers and radioactive ground states. Solenogam is comprised of high-sensitivity γ-ray and electron detector arrays coupled to a new 8-T solenoid. While the installation of the 8-T solenoid proceeds, off-line measurements have been made to characterise Solenogam's performance. Gamma-electron coincidences in the electron capture decay of ^{182}Re into ^{182}W were used to investigate conversion coefficients and γ-e$^-$ angular correlations. The measured conversion coefficients show good agreement with theoretical calculations and have been used to extract $E0/E2$ mixing ratios for a number of $J \rightarrow J$ transitions. The angular correlations measured by the array are in qualitative agreement with theoretical calculations. However, the magnitudes of the correlations are attenuated by approximately 40% for reasons unknown at present. These results are the first full use of the Solenogam system for γ-e$^-$ coincidence measurements and have proven that the system is capable of highly-sensitive internal conversion analysis of complex decays.

1 Introduction

Shape coexistence is a phenomenon observed in nuclei near closed proton and mid neutron shells (e.g $Z \sim 82$, $N \sim 104$). In these nuclei, particle/hole excitations can lead to competing nuclear shapes [1]. One characteristic of coexisting shapes is the presence of multiple rotational bands with different energy spacings dependent on the moment of inertia. Transitions between these rotational structures with $J \rightarrow J$ spin changes are important as they proceed via $E0$, $M1$ and $E2$ components, whose strengths depend strongly on the wavefunctions (and hence shapes) of the initial and final states. As these transitions can proceed with significant $E0$ character, electron spectroscopy is required to fully characterise these transitions.

The current spectrometers available at the ANU-HIAF are the Compton suppressed array (CAESAR) [2] and the Superconducting electron spectrometer (Super-e) [3]. However, neither are suitable for extracting $E0$ strengths from complex data sets. While the CAESAR array is capable of measuring γ-γ coincidences, it lacks the capability for simultaneous measurements of electrons. Conversely, although the Super-e spectrometer can perform e$^-$-e$^-$ coincidence measurements if the electrons are within the acceptance window of the magnet, it is not designed for γ-ray spectroscopy and has only limited e$^-$-γ coincidence capability. The new Solenogam array is capable of combining the benefits of both systems, providing simultaneous access to γ-γ, γ-e$^-$ and e$^-$-e$^-$ coincidences. The array consists of six, 2-mm Si(Li) electron detectors and up to seven γ-ray detectors (including four compton suppressed detectors). Using standard spherical coordinates, the detectors are located at $\phi = 0°, \pm 60°, \pm 120°$, and $180°$ around the beam axis. The Si(Li) detectors are located upstream of the focal point at $\theta = 135°$ to the beam axis while the γ-ray detectors are located downstream at $\theta = 45°$ (A schematic diagram is shown in Fig. 1).

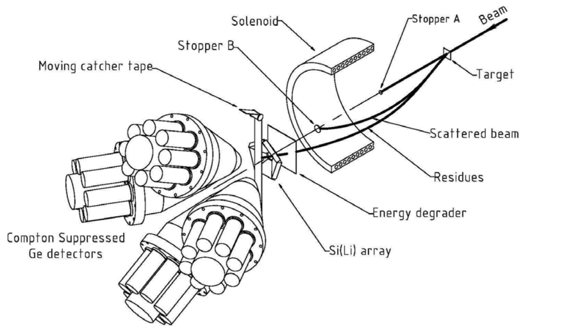

Figure 1. Schematic diagram of the Solenogam system. Note that the three unsuppressed HPGe detectors are not shown.

In the current work, two measurements were made with the array. The first used the Si(Li) array coupled with two high purity germanium (HPGe) gamma-ray detectors. This was subsequently increased to three HPGe and one low energy photon spectrometer (LEPS) detector

[a] e-mail: matthew.gerathy@anu.edu.au

DOI: 10.1051/epjconf/201612304007

for the second measurement. It should be noted that the third HPGe detector had a non-standard placement in the array and was located at $\theta \approx 45°$ and $\phi = 90°$. In both measurements, one of the HPGe detectors was Compton suppressed. Energy resolution in matrices that sum across all detectors are $\approx$ 3 keV (0.2%) for the HPGe detectors and $\approx$ 4 keV (0.4%) for the Si(Li) detectors for the 1408-keV ^{152}Eu decay line and corresponding K conversion line, respectively.

Sources of ^{182}Re with activities of between 1 and 3 μCi were created for offline measurement by the irradiation of 1-mg/cm^2 and 2-mg/cm^2 ^{176}Yb foils. The reaction chosen for this was ^{176}Yb(^{11}B,5n)^{182}Re using 60-MeV ^{11}B ions. The 64-hour halflife of the ^{182}Re parent made offline measurements feasible and measurements were taken for approximately four halflives. During analysis it was found that the 2-mg/cm^2 target was not centred at the focus of the spectrometer, therefore, all spectroscopic data presented here is from the 1 mg/cm^2 source, unless otherwise stated.

2 Results

2.1 ^{182}W

The structure of ^{182}W has been studied extensively with a wide range of spectroscopic information available for comparison [4–11]. A number of rotational structures are populated in the ^{182}Re decay. These are built upon the ground state, and the β (0$^+$), γ (2$^+$), and octupole (3$^-$) vibrations at 0, 1135, 1221 and 1289 keV, respectively. The 4$^-$ band head at 1553 keV is a multi-quasiparticle state [11]. Unfortunately, the excited 0$^+$ state at 1135 keV was not populated in the decay so pure $E0$ transitions were not produced. Gamma-rays were assigned to ^{182}W by comparison with previously measured energies and intensities [9]. Electron lines were assigned using the known tungsten K, L and M binding energies of 69.5, 11.5 and 2.2 keV, respectively [12]. The γ-ray spectrum showed minimal contamination and analysis of characteristic X-rays using the LEPS detector identified tungsten as the major product.

2.2 Spectra and conversion coefficients

The level scheme of ^{182}W is rather complex involving many low-energy transitions (100-400 keV), causing both ungated γ and electron spectra to be contaminated (see Fig. 2). Solenogam, however, is able to isolate clean spectra by imposing γ-ray coincidences. Clean electron lines could only be obtained when gates were placed on coincident γ rays. In particular, gating on the intense yrast transitions could, in many cases, remove the contaminating yrare transitions. Figure 3 shows the electron and γ-ray spectra when gated by the 6$^+$ $\rightarrow$ 4$^+$, 351-keV γ ray of the ground-state band.

Conversion coefficients were obtained for a total of 21 transitions in ^{182}W. The remaining transitions were either too weak, or could not be sufficiently resolved to extract conversion coefficients. The results of the conversion coefficient measurements were compared to theoretical values that were calculated using BrIcc [13]. In general there was good agreement between the measured and theoretical values (see Fig. 4).

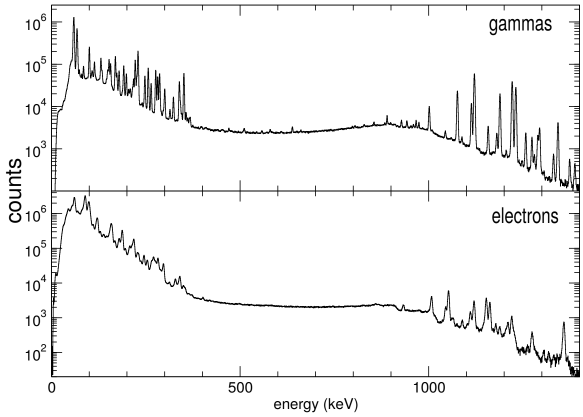

Figure 2. Total projection of γ rays (top) and electrons (bottom) in ^{182}W. Spectra are binned at 0.5 keV/channel

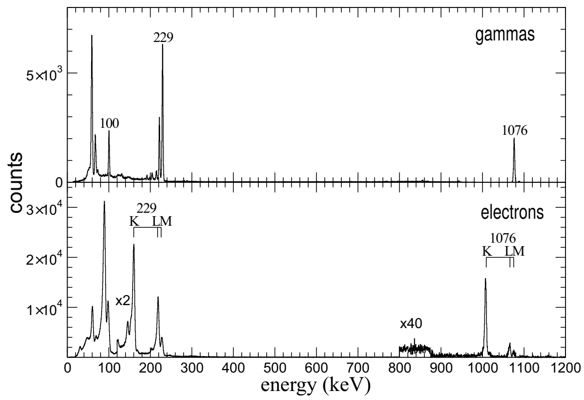

Figure 3. Gamma rays (top) and electrons (bottom) coincident with the 351-keV γ ray. Spectra are binned at 0.5 keV/channel

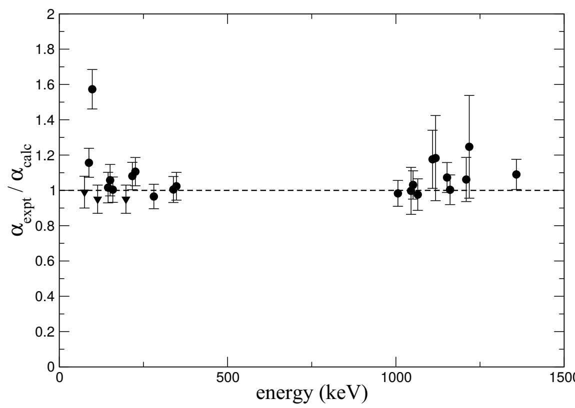

Figure 4. Comparison of measured and theoretical conversion coefficients for ^{182}W (circles) and ^{152}Sm (triangles). Data for ^{152}Sm was obtained with an open calibration source of ^{152}Eu.

Three of the transitions measured were known to have $E0$ admixtures and their $E0/E2$ mixing ratios (q_k) were extracted (see Table 1). The $E0/E2$ mixing ratios evaluated in the current work are in agreement with those previously reported in Ref. [10], however, the large uncertainty means new information cannot be extracted. Nevertheless, the results show the potential power of the Solenogam system.

Table 1. Comparison of $E0/E2$ mixing ratios measured in the current work with values from Ref. [10].

Transition	q_k	
E_γ (keV)	Expt.	Ref. [10]
1076	<0.2	0
1113	<0.4	0.41 (9)
1121	0.21 (16)	0.16 (9)

2.3 Angular correlations

The angular differences between the HPGe and Si(Li) detectors in the Solenogam array and corresponding detector pairs for the current work are given in Table 2.

Table 2. Angular differences and corresponding detector pairs in Solenogam. The notation γ_i and e_j^- refers to the different HPGe and Si(Li) detectors in the array, respectively, and θ_{ij} refers to the angular difference between the detectors.

θ_{ij}	$\cos^2\theta_{ij}$	Detector pairs			
90°	0.0	γ_1, e_3^-	γ_2, e_2^-	γ_3, e_1^-	γ_3, e_4^-
104.5°	0.063	γ_1, e_2^-	γ_1, e_6^-	γ_2, e_1^-	γ_2, e_3^-
120°	0.25	γ_3, e_2^-	γ_3, e_5^-		
138.6°	0.563	γ_1, e_1^-	γ_1, e_5^-	γ_2, e_4^-	γ_2, e_6^-
159°	0.87	γ_3, e_3^-	γ_3, e_6^-		
180°	1.0	γ_1, e_4^-	γ_2, e_5^-		

Angular correlation data was obtained from γ-e$^-$ coincidence matrices constructed for each angular difference in the Solenogam array. Each matrix contained events only from γ-ray and electron detector pairs separated by the corresponding angle. As the array was used with only three HPGe detectors, there were insufficient angular differences between γ-ray detectors to make γ-γ correlation measurements feasible. The γ-e$^-$ angular correlation intensities were extracted by gating on the populating γ-ray in the cascade and measuring the intensity of the depopulating electron and then a Legendre polynomial fit was used to extract A_2 and A_4 values. Typical results are shown in Fig. 5.

Gamma-electron angular correlations were observed for seven of the strongest cascades in ^{182}W (see Table 3). Other cascades were too weak for correlation data to be extracted. The expected angular correlations were calculated using particle parameters b_2 and b_4 from Ref. [14], and mixing ratios from Ref. [9]. There was qualitative agreement between the fitted and the calculated correlations (see Fig. 5), however, Fig. 6 shows that the fitted A_2 values where consistently 40% less then the calculated values. The large uncertainty associated with the fitted A_4 values meant that they where indistinguishable from zero.

Table 3. Angular correlations measured in the current work.

Cascade	Energy (keV)	States involved
1	229-100	$4 \rightarrow 2 \rightarrow 0$
2	1121-100	$2 \rightarrow 2 \rightarrow 0$
3	1342-100	$4 \rightarrow 2 \rightarrow 0$
4	351-229	$6 \rightarrow 4 \rightarrow 2$
5	1427-229	$6 \rightarrow 4 \rightarrow 2$
6	1076-229	$6 \rightarrow 6 \rightarrow 4 \rightarrow 2$
7	1076-351	$6 \rightarrow 6 \rightarrow 4$

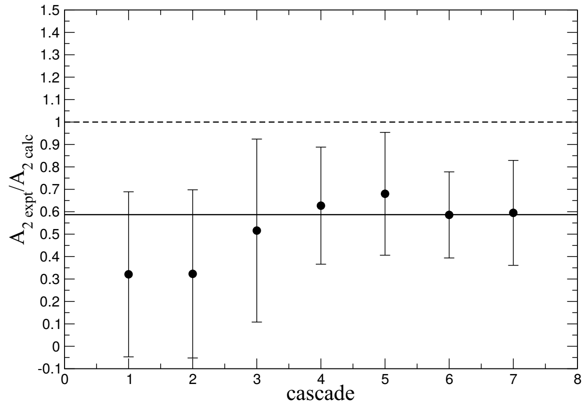

Figure 6. Comparison of measured and theoretical A_2 values. The dashed line at 1 indicates agreement between fitted and calculated values. The solid line at 0.56(10) indicates the weighted average.

The conversion coefficients were first evaluated without correcting for the angular correlation effects, however, the already good agreement with theoretical calculations suggests that the addition of correlations into the evaluation should have minimal effect. Indeed, it had no noticeable effect on the measured conversion coefficients. This result is unsurprising as the wide range of $\cos^2(\theta)$ values sampled in the Solenogam array is expected to average out the correlations. It should be noted that the theoretical correlations were used for these corrections and the observed attenuation was not considered. While this attenuation is still unexplained, it further reduces the impact of the angular correlations on the conversion coefficients.

3 Discussion

The present work has developed Solenogam by using a ^{182}Re source to characterise the performance of the system in obtaining γ-e$^-$ coincidences. These coincidences have been used to study conversion coefficients and γ-e$^-$ angular correlations for selected transitions in ^{182}W. The $E0/E2$ mixing ratios for three $J \rightarrow J$ transitions were evaluated, showing the potential power of the system to probe nuclei that exhibit shape coexistence. The values measured in the current work agree with those previously reported, although, the significant uncertainty means no new information can be extracted. This uncertainty has been attributed to a lack of statistics in the gated-electron spectra, an issue that can be addressed in in-beam experi-

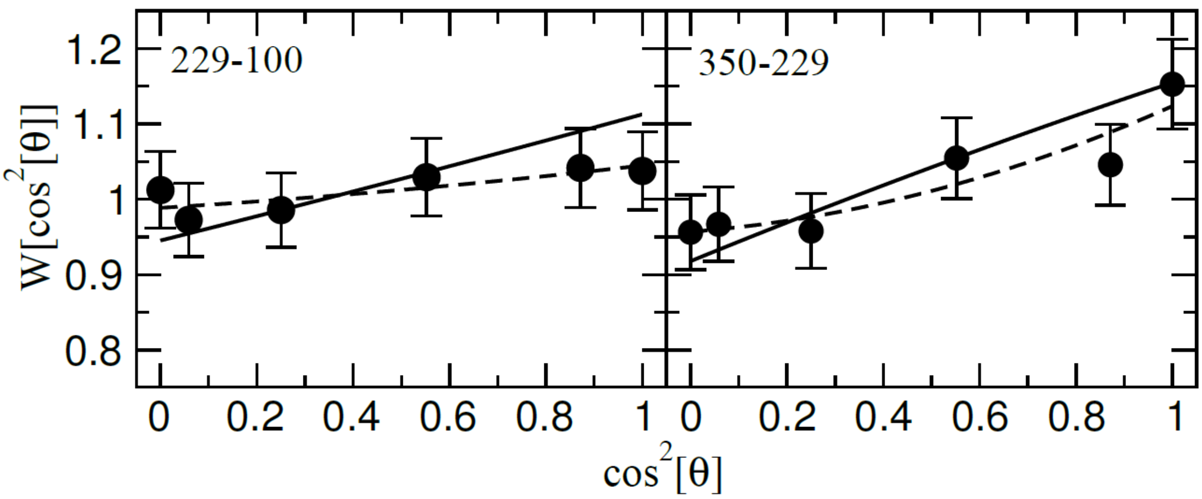

Figure 5. Selected calculated (solid) and observed (dashed) angular correlations in ^{182}W. Cascades are labelled with the energy of the populating γ ray followed by the transition energy for which the conversion electron was observed.

ments where nuclei are continuously produced, in comparison with the present offline source measurement. Of note is that while the $E2/M1$ mixing ratios used in these evaluations were taken from previously reported values, the Solenogam array is able to determine both δ and q_k values. For intense transitions, conversion coefficients can be determined for the K, L and M orbitals, and total conversion coefficients can be independently obtained from γ-γ intensity balances. This will provide ample data to uniquely determine both $E2/M1$ and $E0/E2$ mixing ratios.

The limiting factor for the extraction of conversion coefficients was a lack of suitable γ-ray gates. Many of the yrare transitions could not be isolated by gating and so clean electron spectra were not available. This could be mitigated by requiring triple coincidences, γ-γ-e$^-$ or any such permutation, however, the current setup has a small γ-ray detection efficiency for effective measurement of high-fold events.

Conversion coefficients were measured for transitions with intensity branches as low as 1.56% for low-energy (214 keV) transitions and 4.6% at higher energies (1113 keV). This trend is not unexpected as the probability for internal conversion is less at higher energies leading to weaker electron lines. For L and M electrons, the weakest low-energy transition for which conversion coefficients could be extracted was the 351-keV transition produced in 11.7% of decays. The small uncertainty associated with this value indicates that this is by no means the limit of the system. At higher energies, the 17.4%, 1221-keV transition and the 10.7%, 1076-keV transition were the limits for measuring L and M lines, respectively. However, unlike the 321-keV transition, the large uncertainty associated with the M line of the 1221-keV transition (~20%) indicates that this is approaching the limits of the array in this energy regime.

Solenogam is currently awaiting installation of the 8-T solenoid. Once this process is complete, the system can be used in-beam. This will allow access to nuclei produced using heavy-ion fusion-evaporation reactions. The Solenogam array was originally designed to study shape coexistence in nuclei in the mercury-lead region where neutron-deficient nuclei are only accessible in-beam, however, with further development other areas can be investigated. Indeed, plans are under-way to install six $LaBr_3$(Ce) detectors to enable fast-timing experiments to also be performed with the system.

4 Conclusions

The Solenogam array was used to measure conversion coefficients using γ-e$^-$ coincidences for a range of transitions in ^{182}W and good agreement was achieved with theoretical values. Qualitatively correct angular correlations were observed for a number of cascades, however, these anisotropies were attenuated by approximately 40% for reasons unclear at present. It was further verified that corrections for angular correlation effects were not significant for measuring conversion coefficients. The measurements made in the current work indicate that the Solenogam array has the potential to provide access to a range of interesting nuclei that can be studied in a unique way.

Acknowledgements

This research was supported by the Australian Research Council through grant numbers FT100100991, DP120101417, and DP140103317.

References

[1] K. Heyde and J. L. Wood, Rev. Mod. Phys. **83**, 1467 (2011).

[2] G. D. Dracoulis and A. P. Byrne, Australian National University, Department of Nuclear Physics Annual Report, **ANU-P/1052**, 115 (1989).

DOI: 10.1051/epjconf/201612304007

[3] T. Kibédi, G. D. Dracoulis and A. P. Byrne, Nucl. Instr. Meth. A **294**, 523 (1990).
[4] J. K. Jabber and N. M. Stewart, J. Phys. G **16**, 271 (1990).
[5] D. H. White and R. E. Birkett, Nucl. Phys. **A136**, 657 (1969).
[6] P. H. Regan *et al.*, Nucl. Phys. **A567**, 414 (1994).
[7] J. J. Sapyta, E. G. Funk, and J. W. Mihelich, Nucl. Phys. **A139**, 161 (1969).
[8] M. S. S. El-Daghmah, N. M. Stewart, Z. Phys. A **309**, 219 (1983).
[9] B. Singh, and J. C. Roediger, Nucl. Data Sheets **111** 2081 (2010).
[10] L. Westerberg, L. O. Edvardson, and G. Ch. Madueme, Nucl. Phys. **A255**, 427 (1975).
[11] B. D. Jeltema *et al.*, Nucl. Phys. **A280**, 21 (1977).
[12] G. P. Williams, X-Ray data booklet: Electron binding energies (2000).
[13] T. Kibédi *et al.*, Nucl. Inst. Meth. A **589**, 202 (2008).
[14] R. S. Hager, and E. C. Seltzer, Nucl. Data Sheets. A **4**, 419 (1968).